*Acta Cryst.* (1967). **23**, 549

# The Crystal Structure of $Mn_{15}Si_{26}$

BY H. W. KNOTT, M. H. MUELLER AND L. HEATON

*Argonne National Laboratory, Argonne, Illinois* 60439, *U.S.A.*

(*Received* 27 *September* 1966 *and in revised form* 20 *March* 1967)

X-ray diffraction powder patterns of Mn–Si alloys over the range MnSi to $MnSi_2$ have indicated a phase of approximate $MnSi_{1\cdot7}$ composition. Rotation film patterns and diffractometer intensities, using an orienter technique, were also obtained from a single crystal of $MnSi_{1\cdot75}$. Results from examining over 2000 reflections were used in Patterson, Fourier and least-squares methods in establishing the structure. The compound found, $Mn_{15}Si_{26}$, is tetragonal, $a=5\cdot531$, $c=65\cdot311$ Å, space group $I\bar{4}2d$, $Z=4$, and 8 Mn and 7 Si atoms in the asymmetric unit. The unit cell consists of 15 stacked small Mn subcells with 52 Si atom pairs oriented alternately in opposite quadrants about the central axis in the **c** direction. The structure may also be described as pseudo-hexagonal sheets along and parallel to {110}. Comparisons are made with other reported structures.

## Introduction

$MnSi_2$, which was considered a type structure, has been reported by Borén (1933) as a tetragonal cell with $a=5\cdot524$, $c=17\cdot457$ Å. Korshunov, Siderenko, Gel'd & Davydov (1961), after investigating the Mn–Si system, stated that the true composition of the phase must be in the region $MnSi_{1\cdot67}$ to $MnSi_{1\cdot73}$. Schwomma, Nowotny & Wittman (1963) reported the composition as $MnSi_{\sim1\cdot7}$, and the unit cell as tetragonal with $a=5\cdot518$, $c=48\cdot136$ Å. Investigation of the phase diagram by Fujino, Shinoda, Asanabe & Sasaki indicated an $MnSi_{1\cdot72}$ phase which appeared to fit a tetragonal cell of $a=5\cdot526$, $c=17\cdot455$ Å. Schwomma, Preisinger, Nowotny & Wittman (1964), continuing their previous study, reported the space group, $P\bar{4}n2$, and atom positions for $Mn_{11}Si_{19}$. Mueller & Knott (1965) reported $Mn_4Si_7$ as a tetragonal cell with $a=5\cdot524$, $c=17\cdot46$ Å, and the space group as $P\bar{4}c2$. A. Brown at the University of Uppsala, cited by Aronsson, Lundström & Rundqvist (1965), reported a tetragonal cell with an $a$ of 5·49 Å and an even longer $c$ of 112·42 Å for $MnSi_{1\cdot7}$.

At the time the initial investigation of this structure was undertaken at Argonne, we were unaware of the above publication by Schwomma *et al.* (1963) reporting a unit cell with a longer $c$. Our concurrent investigation indicated that a $c$ of 17·46 Å was sufficient to define the cell, as judged by the good agreement of $F_{obs}$ and $F_{calc}$ of over 300 nonequivalent reflections giving an $R$ value of 7·7%. However, in view of the reported longer cell, it was decided to re-evaluate our original data and to collect an additional set of data from another single crystal. As a result of this reinvestigation, it was found that both of our crystals could be described best as a tetragonal cell with $c=65\cdot311$ Å. This paper will define the structure based on the 65 Å length cell and a comparison will be made of the structures of different lengths with the slight differences pointed out.

A series of compounds in the range $TB_{1\cdot25}$ to $TB_2$, where T is a transition metal of Groups V, VI, VII, or VIII, and B is an element of Groups III or IV has been reported by Wittman & Nowotny (1965); Darby, Downey & Norton (1965); Jeitschko & Parthé (1967); and Vollenke, Preisinger, Nowotny & Wittman (1967). A few of the compounds are ternary alloys in which either the T or B component consists of varying amounts of two elements. These all appear to be similar to the manganese–silicon phase under discussion in that all are tetragonal cells with an $a$ around 6 Å and unusually long $c$'s, up to 300 Å.

## Experimental

Manganese–silicon alloys of varying composition were made from electrolytic manganese of 99·5% purity and silicon of 99·98% purity in an arc melting furnace. They were annealed for homogenization one week at 750 °C and water quenched. Since these alloys were very brittle the cast buttons were crushed and a small portion ground giving a suitable material for X-ray powder patterns. Small fragments were examined by X-ray techniques in order to select a single crystal. The results of the powder patterns, as shown in Table 1, indicate that the phase is near a composition of $MnSi_{1\cdot74}$. Powder patterns of this material were indexed according to the small tetragonal cell with $c=17\cdot46$ Å. However, rotation patterns obtained from a single crystal ($0\cdot042\times0\cdot014\times0\cdot500$ mm) of an $MnSi_{1\cdot75}$ alloy showed some discrepancies from the small cell and indicated a true $c$ of 15/4 times the original value, or about 65·5 Å. A re-evaluation of an earlier rotation pattern from a single crystal removed from a two phase $MnSi_2$ alloy also agreed best with this long $c$ of 65·5 Å. New lattice constants, based on the larger cell, were obtained from the powder pattern with an Argonne least-squares lattice constant program, B-106, which is a modification of the original MET-124 version of this program (Mueller, Heaton & Miller, 1960).

Table 1. *Identification of the partial manganese–silicon system by X-ray diffraction**

| Composition | Phases identified |
|---|---|
| MnSi | MnSi |
| $MnSi_{1\cdot72}$ | Tet. + weak MnSi |
| $MnSi_{1\cdot74}$ | Tet. |
| $MnSi_{1\cdot75}$ | Tet. + v. weak Si |
| $MnSi_{1\cdot76}$ | Tet. + weak Si |
| $MnSi_{1\cdot78}$ | Tet. + weak Si |
| $MnSi_2$ | Tet. + Si |

* All patterns are from powder samples in 114·59 mm diameter Debye–Scherrer cameras exposed to filtered chromium radiation.

Since this cell is extremely long in the **c** direction and there were a large number of unobserved reflections, the possibility of twinning should be considered. This was investigated by examining large polished sections of this alloy at 500 to 2000 magnification with reflected polarized light. Small fragments selected as single crystals were also examined; however, there was no evidence for twinning in either case.

Angular positions for 8000 general reflections in one octant up to 82° $2\theta$ for molybdenum radiation were obtained with an Argonne least-squares crystallographic orientation program, B-101. Intensity measurements and background readings were then made with a single crystal mounted on a single-crystal orienter using a stationary-crystal stationary-counter technique. After the first 2000 reflections produced no intensity on non-body-centered reflections, additional observations were confined to body-centered data only. A total of 605 reciprocal lattice points within one octant had observed intensity. Of these the 36 strongest reflections, between 14000 and 68000 c.p.s., were adjusted to compensate for saturation of the scintillation counter. There was no resolution of the peaks from the Mo $K\alpha$ doublet up to 82° $2\theta$. Twenty random *hkl*'s between 20° and 80° were compared for integrated *versus* peak intensity, and as a result of this comparison a correction was applied to the peak intensity of reflections greater than 62° $2\theta$ to compensate for the drop-off of intensity due to the stationary-crystal stationary-counter method. No correction was made for absorption since Mo radiation was used, in which the correction was very small for the majority of these observations, as evidenced by the good agreement with equivalent reflections in the various octants.

Since there were a large number of $F$'s observed with zero intensity, as indicated previously, the possibility existed that many reflections were accidentally absent from composition and/or unique positions and not because of space group restrictions. Hence at this point it was decided to use all 605 $F^2$'s as independent reflections. The 3-D Patterson map from an Argonne adaptation of the Sly–Shoemaker Fourier program, B-114 (Sly & Shoemaker, 1960), was obtained on the basis of the lower tetragonal Laue symmetry, $4/m$ rather than $4/mmm$, and all space groups which were possible based on either symmetry were considered. For the observed reflections the Laue symmetry appeared to be $4/mmm$ and the following restrictions applied: $hkl$, $h+k+l=2n$; $hhl$, $2h+l=4n$; and with one weak exception (310), $hk0$, $h,k=2n$. For the first two restrictions, the possible space groups are $I4_1md$ and $I\bar{4}2d$. If, in addition, the third restriction is true, then $I4_1/amd$ is possible. After our initial peak intensity measurements were made, however, $2\theta$ scans along certain $hk0$ reciprocal lattice rows with $h,k=2n+1$ were made in order to establish if this last restriction applied. Very small but significant intensity was observed for at least three other reflections of this kind indicating that $hk0$ with $h$ and $k$ odd appear.

If none of the restrictions are necessarily due to the space group, then seven tetragonal groups are possible, based on the probable manganese arrangement obtained from the Patterson map and the minimum Si–Si distance possible. These seven space groups are $I4_1$, $P\bar{4}$, $I\bar{4}$, $I4_1/a$, $I4_122$, $P\bar{4}n2$, and $I\bar{4}2d$. These are the only seven possible groups from the standpoint of spatial considerations, regardless of observed extinctions. Any other space group would necessitate some Mn–Mn distances as low as 2·1 Å or some Si–Si distances as low as 1·8 Å. Two of the first three space groups considered above from the standpoint of observed extinctions, $I4_1md$ and $I4_1/amd$, were eliminated by spatial considerations and the symmetry of the Patterson map. Structure factors for the seven remaining space groups were calculated using elemental form factors from *International Tables for X-ray Crystallography* (1962) and were compared with $F_{obs}$ data in MET-153, the Argonne version of the Fortran Crystallographic Least-Squares Program (Busing, Martin & Levy, 1962). Four groups had initial agreement factors greater than 30%. Further study indicated that these were unacceptable because they required occasional Mn–Si distances as short as 1·4 Å. The remaining three space groups, $P\bar{4}$, $I\bar{4}$, and $I\bar{4}2d$, had initial $R$ values under 15%, and the shortest interatomic distances necessary were 2·3 Å. Of all the space groups discussed, only $I\bar{4}2d$ was acceptable because it had all of the following: $4/mmm$ Laue symmetry, the two observed extinction conditions, no interatomic distances less than 2·3 Å, and complete agreement with the Patterson map. It was not necessary to go to $I\bar{4}$ or $P\bar{4}$, which were less symmetrical cases of $I\bar{4}2d$. The 605 reflections with observed intensity utilized in the Patterson function and preliminary least-squares trials were reduced by averaging appropriate pairs to 371 nonequivalent reflections. A three-dimensional Fourier map of $I\bar{4}2d$ verified the atom positions, and these were then refined with a least-squares technique. A difference Fourier using the refined positional parameters based on this space group was devoid of prominences.

Considerable difficulty was encountered in the crystallographic least-squares program owing to some unique conditions. Many of the attempts at parameter refinement were stalled by singular matrix stops. These

were due to the fact that many of the atoms in the asymmetric unit had values for variable positional parameters that tended to interact and produce near zero diagonal elements in the matrix. It was necessary either to allow only selected groups of atoms to vary position or to pick particular starting positions within each group that would not produce computer stops. The other frequently occurring difficulty was the over-correction of variables, due to the long $c$ (65 Å), large $l$ index (up to 120), and the limited distribution of $l$'s (only 50 observed between $l=0$ and $l=120$). This caused successive attempts at refinement of the parameters to produce diverging $R$ values. It was overcome by modifying MET-153 to produce a selective partial shifts of any variable.

This structure offered a dramatic example of the effect of accidentally absent reflections on the $R$ value. The final unweighted $R$ of 371 observed reflections was 0·044. There were, in addition, 1548 accidentally absent reflections. If these 1548 reflections were added with $F_{obs}=0$ to the 371 reflections with $F_{obs}>0$, then $R$ for 1919 reflections would be 0·750. However, of the 1548 absent reflections 1290 had an $F_{calc}$ less than $F_{Lim}$, where $F_{Lim}$ is a variable number determined from a constant $I_{min}$ of the counting equipment. When these 1290 reflections were removed, the $R$ for the remaining 629 reflections was 0·274. If $F_{obs}$ for the 258 reflections observed as zero is set equal to $F_{Lim}$, the $R$ value for 629 reflections is 0·086. The 1548 accidentally absent reflections were given zero weight in the least-squares refinement. Observed and calculated structure factors for the 371 observed reflections are listed in Table 2.

## Description of the structure

The $4(Mn_{15}Si_{26})$ cell is composed of 15 almost identical subcells of 4 manganese atoms each, stacked atop each other in the **c** direction. Seven and a half of these are shown in Fig. 1(*a*). The manganese atoms spiral up the cell in the following manner: 0,0,0; $\frac{1}{2}$,0, ~1/60; $\frac{1}{2}$,$\frac{1}{2}$, ~2/60; 0,$\frac{1}{2}$, ~3/60; 0,0, ~4/60; $\frac{1}{2}$,0, ~5/60; *etc.* Within the cell there are 52 silicon atom pairs at $x$ and $y$ coordinates near $\pm\frac{1}{6}$ or $\pm\frac{1}{3}$ and $z$ coordinates near $(2n-1)/104$, where $n$ is 1 through 52. These 52 silicon atom pairs may be thought of as a dumbbell arrangement about the central axis of the tetragonal cell oriented alternately in opposite quadrants about the central axis in the **c** direction. Half of these silicon atom pairs are shown in Fig. 1(*b*). Fig. 1(*c*) is a composite of the first two drawings, showing all atoms for one-half the cell. Finally, in Fig. 1(*d*) about half the atoms are preferentially removed to show the near hexagonal, near planar array of the atoms along the (110) and (1$\bar{1}$0) planes. The atoms removed lie in a similar array in or near the (220) and (2$\bar{2}$0) planes. A 90° rotation of all these planes occurs at every one-eighth $z$, which occurs four times in the half cell as shown. The (110) planar arrangement between $z=0$ and $z=\frac{1}{8}$ becomes

Table 2. *Observed and calculated structure factors*

| H | K | L | FOBS | FCAL | H | K | L | FOBS | FCAL | H | K | L | FOBS | FCAL | H | K | L | FOBS | FCAL | H | K | L | FOBS | FCAL | H | K | L | FOBS | FCAL |
|---|---|---|---|---|---|---|---|---|---|---|---|---|---|---|---|---|---|---|---|---|---|---|---|---|---|---|---|---|---|
| 2 | 0 | 0 | 676 | 683 | 5 | 2 | 11 | 81 | 79 | 5 | 0 | 23 | 122 | 117 | 5 | 1 | 38 | 64 | 64 | 2 | 1 | 53 | 82 | 85 | 2 | 1 | 75 | 356 | 351 |
| 4 | 0 | 0 | 692 | 635 | 7 | 2 | 11 | 103 | 94 | 7 | 0 | 23 | 86 | 82 | 7 | 1 | 38 | 102 | 104 | 4 | 1 | 53 | 82 | 81 | 4 | 1 | 75 | 309 | 313 |
| 6 | 0 | 0 | 954 | 927 | 4 | 3 | 11 | 89 | 93 | 9 | 0 | 23 | 91 | 96 | 3 | 3 | 38 | 99 | 104 | 3 | 2 | 53 | 81 | 90 | 6 | 1 | 75 | 196 | 253 |
| 8 | 0 | 0 | 381 | 392 | 5 | 4 | 11 | 77 | 79 | 2 | 1 | 23 | 69 | 81 | 5 | 3 | 38 | 88 | 95 | 5 | 2 | 53 | 67 | 71 | 3 | 2 | 75 | 251 | 268 |
| 10 | 0 | 0 | 286 | 302 | 7 | 4 | 11 | 82 | 78 | 4 | 1 | 23 | 77 | 87 | 9 | 3 | 38 | 114 | 113 | 3 | 1 | 56 | 89 | 94 | 5 | 2 | 75 | 251 | 268 |
| 3 | 1 | 0 | 36 | 32 | 4 | 0 | 14 | 47 | 49 | 3 | 2 | 23 | 49 | 49 | 2 | 1 | 41 | 375 | 373 | 5 | 1 | 56 | 114 | 115 | 7 | 2 | 75 | 277 | 280 |
| 2 | 2 | 0 | 1213 | 1276 | 6 | 0 | 14 | 63 | 65 | 6 | 3 | 23 | 103 | 105 | 4 | 1 | 41 | 297 | 273 | 2 | 2 | 56 | 297 | 284 | 4 | 3 | 75 | 240 | 257 |
| 4 | 2 | 0 | 979 | 980 | 8 | 0 | 14 | 77 | 58 | 7 | 4 | 23 | 109 | 112 | 8 | 1 | 41 | 110 | 115 | 4 | 2 | 56 | 256 | 246 | 6 | 3 | 75 | 301 | 311 |
| 6 | 2 | 0 | 379 | 367 | 3 | 3 | 14 | 56 | 64 | 1 | 1 | 26 | 671 | 690 | 3 | 2 | 41 | 97 | 107 | 4 | 4 | 56 | 216 | 210 | 5 | 4 | 75 | 213 | 228 |
| 8 | 2 | 0 | 469 | 479 | 1 | 0 | 15 | 560 | 511 | 3 | 1 | 26 | 84 | 84 | 5 | 2 | 41 | 102 | 92 | 5 | 3 | 56 | 69 | 76 | 6 | 5 | 75 | 244 | 252 |
| 10 | 2 | 0 | 457 | 494 | 3 | 0 | 15 | 1119 | 1187 | 5 | 1 | 26 | 301 | 282 | 7 | 2 | 41 | 80 | 76 | 4 | 3 | 56 | 114 | 121 | 1 | 1 | 78 | 273 | 271 |
| 4 | 4 | 0 | 592 | 552 | 5 | 0 | 15 | 341 | 333 | 7 | 1 | 26 | 180 | 168 | 5 | 4 | 41 | 110 | 106 | 0 | 0 | 60 | 840 | 791 | 5 | 1 | 78 | 128 | 129 |
| 6 | 4 | 0 | 508 | 498 | 7 | 0 | 15 | 222 | 219 | 5 | 3 | 26 | 125 | 119 | 0 | 0 | 44 | 127 | 134 | 2 | 0 | 60 | 553 | 538 | 7 | 1 | 78 | 93 | 94 |
| 8 | 4 | 0 | 462 | 467 | 9 | 0 | 15 | 400 | 419 | 3 | 0 | 29 | 87 | 88 | 2 | 0 | 44 | 71 | 60 | 4 | 0 | 60 | 402 | 390 | 1 | 1 | 82 | 87 | 113 |
| 6 | 6 | 0 | 923 | 939 | 2 | 1 | 15 | 885 | 941 | 5 | 0 | 29 | 64 | 60 | 4 | 0 | 44 | 61 | 65 | 6 | 0 | 60 | 576 | 577 | 3 | 1 | 82 | 273 | 271 |
| 8 | 6 | 0 | 341 | 334 | 4 | 1 | 15 | 596 | 561 | 3 | 2 | 29 | 39 | 39 | 2 | 2 | 44 | 52 | 58 | 8 | 0 | 60 | 278 | 283 | 7 | 1 | 82 | 110 | 110 |
| 2 | 1 | 3 | 28 | 30 | 6 | 1 | 15 | 350 | 338 | 2 | 0 | 30 | 105 | 107 | 4 | 2 | 44 | 93 | 90 | 2 | 2 | 60 | 593 | 581 | 3 | 3 | 82 | 99 | 85 |
| 4 | 1 | 3 | 61 | 58 | 8 | 1 | 15 | 336 | 351 | 4 | 0 | 30 | 218 | 220 | 6 | 2 | 44 | 88 | 97 | 4 | 2 | 60 | 523 | 517 | 5 | 3 | 82 | 228 | 237 |
| 6 | 1 | 3 | 76 | 74 | 10 | 1 | 15 | 273 | 280 | 6 | 0 | 30 | 128 | 126 | 1 | 0 | 45 | 515 | 484 | 6 | 2 | 60 | 340 | 360 | 1 | 0 | 83 | 82 | 87 |
| 5 | 2 | 3 | 61 | 59 | 3 | 2 | 15 | 328 | 306 | 1 | 1 | 30 | 1001 | 1130 | 8 | 2 | 60 | 376 | 392 | 3 | 0 | 45 | 696 | 674 | 3 | 0 | 83 | 66 | 65 |
| 7 | 2 | 3 | 77 | 80 | 5 | 2 | 15 | 557 | 520 | 3 | 1 | 30 | 613 | 573 | 5 | 0 | 45 | 256 | 222 | 5 | 3 | 60 | 78 | 78 | 2 | 1 | 83 | 80 | 94 |
| 9 | 2 | 3 | 99 | 97 | 7 | 2 | 15 | 468 | 458 | 5 | 1 | 30 | 747 | 719 | 7 | 0 | 45 | 374 | 374 | 7 | 3 | 60 | 96 | 100 | 3 | 2 | 83 | 68 | 81 |
| 8 | 3 | 3 | 94 | 91 | 9 | 2 | 15 | 189 | 207 | 7 | 1 | 30 | 501 | 505 | 9 | 0 | 45 | 272 | 276 | 4 | 4 | 60 | 507 | 524 | 1 | 1 | 86 | 114 | 111 |
| 3 | 1 | 4 | 207 | 195 | 4 | 3 | 15 | 483 | 456 | 9 | 1 | 30 | 324 | 350 | 2 | 1 | 45 | 553 | 593 | 6 | 4 | 60 | 263 | 287 | 5 | 1 | 86 | 101 | 109 |
| 5 | 1 | 4 | 226 | 212 | 6 | 3 | 15 | 527 | 504 | 4 | 2 | 30 | 133 | 130 | 4 | 1 | 45 | 553 | 529 | 8 | 4 | 60 | 480 | 476 | 7 | 1 | 86 | 103 | 83 |
| 2 | 2 | 4 | 368 | 372 | 8 | 3 | 15 | 233 | 253 | 6 | 2 | 30 | 100 | 99 | 6 | 1 | 45 | 240 | 244 | 2 | 1 | 63 | 214 | 216 | 5 | 5 | 86 | 119 | 106 |
| 4 | 2 | 4 | 313 | 322 | 5 | 4 | 15 | 468 | 441 | 3 | 3 | 30 | 1062 | 1103 | 8 | 1 | 45 | 285 | 305 | 4 | 1 | 63 | 132 | 132 | 1 | 0 | 89 | 76 | 75 |
| 6 | 2 | 4 | 97 | 94 | 7 | 4 | 15 | 274 | 280 | 5 | 3 | 30 | 383 | 381 | 3 | 2 | 45 | 435 | 423 | 6 | 1 | 63 | 124 | 116 | 3 | 0 | 89 | 108 | 111 |
| 5 | 3 | 4 | 107 | 99 | 9 | 4 | 15 | 279 | 281 | 7 | 3 | 30 | 173 | 186 | 5 | 2 | 45 | 430 | 424 | 3 | 2 | 63 | 93 | 100 | 3 | 2 | 89 | 87 | 92 |
| 4 | 4 | 4 | 263 | 244 | 6 | 5 | 15 | 255 | 257 | 9 | 3 | 30 | 483 | 479 | 7 | 2 | 45 | 242 | 260 | 1 | 0 | 67 | 291 | 276 | 1 | 1 | 90 | 385 | 401 |
| 8 | 4 | 4 | 98 | 96 | 8 | 5 | 15 | 291 | 301 | 5 | 5 | 30 | 528 | 528 | 9 | 2 | 45 | 257 | 267 | 3 | 0 | 67 | 201 | 180 | 3 | 1 | 90 | 308 | 329 |
| 1 | 0 | 7 | 78 | 70 | 7 | 6 | 15 | 275 | 280 | 7 | 5 | 30 | 468 | 473 | 4 | 3 | 45 | 191 | 192 | 5 | 0 | 67 | 218 | 210 | 5 | 1 | 90 | 328 | 333 |
| 3 | 0 | 7 | 109 | 105 | 1 | 1 | 18 | 74 | 70 | 7 | 7 | 30 | 342 | 341 | 6 | 3 | 45 | 490 | 501 | 7 | 0 | 67 | 111 | 125 | 3 | 3 | 90 | 378 | 383 |
| 5 | 0 | 7 | 192 | 181 | 3 | 1 | 18 | 56 | 65 | 4 | 1 | 33 | 64 | 66 | 8 | 3 | 45 | 222 | 239 | 4 | 1 | 67 | 77 | 91 | 5 | 3 | 90 | 293 | 315 |
| 7 | 0 | 7 | 95 | 91 | 5 | 1 | 18 | 68 | 70 | 6 | 1 | 33 | 107 | 111 | 5 | 4 | 45 | 427 | 424 | 6 | 1 | 67 | 123 | 126 | 2 | 1 | 93 | 131 | 132 |
| 2 | 1 | 7 | 76 | 67 | 4 | 2 | 18 | 72 | 75 | 3 | 2 | 33 | 139 | 142 | 7 | 4 | 45 | 276 | 295 | 3 | 2 | 67 | 258 | 258 | 4 | 1 | 93 | 122 | 124 |
| 4 | 1 | 7 | 119 | 119 | 6 | 2 | 18 | 116 | 117 | 5 | 2 | 33 | 162 | 162 | 6 | 5 | 45 | 169 | 189 | 4 | 3 | 67 | 128 | 129 | 1 | 0 | 97 | 163 | 165 |
| 6 | 1 | 7 | 111 | 108 | 5 | 3 | 18 | 83 | 83 | 4 | 3 | 33 | 88 | 90 | 8 | 5 | 45 | 269 | 265 | 7 | 4 | 67 | 110 | 108 | 5 | 0 | 97 | 181 | 177 |
| 7 | 2 | 7 | 89 | 90 | 6 | 4 | 18 | 99 | 96 | 5 | 4 | 33 | 146 | 153 | 7 | 6 | 45 | 254 | 257 | 6 | 5 | 67 | 142 | 142 | 2 | 1 | 97 | 84 | 95 |
| 4 | 3 | 7 | 253 | 240 | 5 | 5 | 18 | 162 | 157 | 1 | 1 | 34 | 73 | 83 | 3 | 1 | 48 | 146 | 147 | 8 | 0 | 68 | 123 | 123 | 6 | 1 | 97 | 159 | 150 |
| 6 | 3 | 7 | 174 | 170 | 7 | 5 | 18 | 85 | 89 | 3 | 1 | 34 | 41 | 54 | 5 | 1 | 48 | 168 | 165 | 2 | 0 | 68 | 129 | 128 | 3 | 2 | 97 | 135 | 144 |
| 5 | 4 | 7 | 97 | 91 | 2 | 1 | 19 | 101 | 93 | 5 | 1 | 34 | 136 | 135 | 2 | 2 | 48 | 165 | 177 | 4 | 0 | 68 | 94 | 105 | 4 | 3 | 97 | 173 | 175 |
| 6 | 5 | 7 | 117 | 114 | 4 | 1 | 19 | 164 | 165 | 7 | 1 | 34 | 107 | 106 | 4 | 2 | 48 | 139 | 147 | 6 | 0 | 68 | 84 | 90 | 1 | 1 | 98 | 103 | 121 |
| 0 | 0 | 8 | 98 | 90 | 6 | 1 | 19 | 139 | 126 | 4 | 2 | 34 | 77 | 78 | 6 | 2 | 48 | 80 | 86 | 8 | 0 | 68 | 101 | 90 | 3 | 1 | 98 | 101 | 111 |
| 2 | 0 | 8 | 56 | 61 | 3 | 2 | 19 | 131 | 140 | 6 | 2 | 34 | 123 | 125 | 4 | 4 | 48 | 139 | 119 | 2 | 2 | 68 | 118 | 116 | 5 | 1 | 98 | 103 | 103 |
| 4 | 0 | 8 | 97 | 98 | 5 | 2 | 19 | 232 | 228 | 8 | 2 | 34 | 83 | 82 | 2 | 1 | 49 | 51 | 44 | 4 | 2 | 68 | 98 | 107 | 3 | 3 | 98 | 97 | 88 |
| 6 | 0 | 8 | 160 | 161 | 7 | 2 | 19 | 102 | 102 | 8 | 4 | 34 | 101 | 101 | 6 | 1 | 49 | 80 | 76 | 6 | 2 | 68 | 84 | 95 | 5 | 3 | 98 | 106 | 93 |
| 3 | 1 | 8 | 34 | 37 | 4 | 3 | 19 | 96 | 101 | 8 | 4 | 34 | 93 | 94 | 5 | 2 | 49 | 66 | 69 | 4 | 4 | 68 | 100 | 105 | 0 | 0 | 104 | 188 | 176 |
| 5 | 1 | 8 | 83 | 81 | 5 | 4 | 19 | 224 | 210 | 5 | 5 | 34 | 178 | 174 | 7 | 2 | 49 | 86 | 88 | 1 | 1 | 70 | 80 | 103 | 2 | 0 | 104 | 98 | 91 |
| 7 | 1 | 8 | 70 | 73 | 7 | 4 | 19 | 103 | 96 | 7 | 5 | 34 | 103 | 106 | 0 | 0 | 52 | 482 | 505 | 2 | 1 | 71 | 108 | 101 | 1 | 0 | 105 | 201 | 210 |
| 2 | 2 | 8 | 48 | 52 | 2 | 0 | 22 | 145 | 139 | 1 | 0 | 37 | 353 | 339 | 2 | 0 | 52 | 494 | 482 | 4 | 1 | 71 | 141 | 129 | 3 | 0 | 105 | 221 | 230 |
| 4 | 2 | 8 | 41 | 48 | 4 | 0 | 22 | 268 | 281 | 3 | 0 | 37 | 306 | 310 | 4 | 0 | 52 | 260 | 250 | 5 | 2 | 71 | 141 | 147 | 5 | 0 | 105 | 182 | 183 |
| 6 | 2 | 8 | 118 | 114 | 6 | 0 | 22 | 139 | 138 | 5 | 0 | 37 | 139 | 134 | 6 | 0 | 52 | 137 | 115 | 7 | 2 | 71 | 86 | 86 | 2 | 1 | 105 | 201 | 214 |
| 8 | 2 | 8 | 122 | 115 | 10 | 0 | 22 | 105 | 94 | 7 | 0 | 37 | 209 | 204 | 8 | 0 | 52 | 134 | 137 | 5 | 4 | 71 | 133 | 139 | 4 | 1 | 105 | 217 | 219 |
| 7 | 3 | 8 | 134 | 135 | 3 | 1 | 22 | 275 | 262 | 2 | 1 | 37 | 75 | 70 | 2 | 2 | 52 | 75 | 66 | 2 | 0 | 74 | 66 | 64 | 3 | 2 | 105 | 196 | 212 |
| 6 | 4 | 8 | 161 | 159 | 4 | 2 | 22 | 166 | 165 | 4 | 1 | 37 | 93 | 93 | 6 | 2 | 52 | 234 | 236 | 4 | 0 | 74 | 130 | 131 | 4 | 3 | 105 | 169 | 172 |
| 6 | 4 | 8 | 122 | 115 | 6 | 2 | 22 | 115 | 113 | 6 | 1 | 37 | 108 | 106 | 4 | 4 | 52 | 157 | 161 | 4 | 2 | 74 | 81 | 85 | 2 | 2 | 108 | 123 | 119 |
| 6 | 6 | 8 | 152 | 153 | 3 | 3 | 22 | 259 | 267 | 3 | 2 | 37 | 126 | 129 | 6 | 4 | 52 | 93 | 96 | 3 | 3 | 74 | 84 | 85 | 4 | 2 | 108 | 128 | 113 |
| 2 | 1 | 11 | 484 | 470 | 5 | 3 | 22 | 190 | 184 | 5 | 2 | 37 | 125 | 120 | 1 | 0 | 53 | 96 | 91 | 1 | 0 | 75 | 299 | 291 | 2 | 0 | 112 | 207 | 203 |
| 4 | 1 | 11 | 323 | 312 | 7 | 3 | 22 | 103 | 102 | 8 | 3 | 37 | 104 | 102 | 3 | 0 | 53 | 92 | 90 | 3 | 0 | 75 | 388 | 376 | 2 | 2 | 112 | 119 | 126 |
| 6 | 1 | 11 | 71 | 69 | 1 | 0 | 23 | 59 | 48 | 1 | 1 | 38 | 137 | 148 | 5 | 0 | 53 | 61 | 61 | 5 | 0 | 75 | 295 | 282 | 0 | 0 | 120 | 290 | 283 |
| 8 | 1 | 11 | 164 | 163 | 3 | 0 | 23 | 57 | 56 | 3 | 1 | 38 | 93 | 90 | 9 | 0 | 53 | 98 | 100 | 7 | 0 | 75 | 141 | 154 | | | | | |
| 3 | 2 | 11 | 165 | 151 | | | | | | | | | | | | | | | | | | | | | | | | | |

the (220) planar arrangement between $z=\frac{2}{8}$ and $z=\frac{3}{8}$. In a similar manner the $(1\bar{1}0)$ arrangement between $z=\frac{1}{8}$ and $z=\frac{2}{8}$ becomes the $(2\bar{2}0)$ arrangement between $z=\frac{3}{8}$ and $z=\frac{4}{8}$. Thus, along the $\langle 110\rangle$ and $\langle 1\bar{1}0\rangle$ directions, the planes are arranged in an *ABAB* pattern. The greatest distortion of the planes and the longest Si–Si distances occur near each one-eighth of $z$ where the planes rotate.

The atom positions and the values obtained for their parameters are listed in Table 3. No standard errors are listed for the temperature factors because the apparent errors are large. This is due to the fact that temperature factors for eight different manganese groups or for seven different silicon groups are difficult to obtain. For instance, eight different manganese groups whose $z$ parameters are almost small multiples of each other produce only three groups of structure factors for sixty manganese atoms as follows: when $l=30n$, $F_{Mn}\sim 60f_{Mn}$; when $l=30n+15$, $F_{Mn}\sim 30\sqrt{2}f_{Mn}$; and when $l\neq 15n$, $F_{Mn}\sim 0$. For any specific reflection, all the individual $f_{Mn}$ in the first group are essentially equal to each other, all the individual $f_{Mn}$ in the second category are nearly equal to each other, and the net result of all the individual $f_{Mn}$ in the third category is almost zero. To a slightly lesser degree the same problem pertains to seven silicon groups. Hence, it is more practical to consider an average $B_{Mn}=0{\cdot}17$ and $B_{Si}=0{\cdot}39$, as obtained from the values in Table 3.

Interatomic distances were obtained after the final refinement of the positional parameters from B-115, an Argonne adaptation of the Fortran Crystallographic Function and Error Program (Busing, Martin & Levy, 1964). The number of nearest neighbors for Mn–Mn and Mn–Si were satisfactorily established but could not be conclusively resolved for Si–Si, since there was a considerable spread of distances as shown in Fig. 2. All Si–Si distances up to 4 Å are reported. Since most atoms are surrounded by many neighbors each at slightly different distances, only the range of distances between each atom and its neighbors is listed in Table 4.

The manganese–silicon distances present in this structure – as low as 2·27 Å – are significantly below the reported elemental distances for Mn (2·73 Å) and Si (2·35 Å), and these short Mn–Si distances indicate some covalent bonding. Bonding and packing in this structure must have an important role in the large cell size.

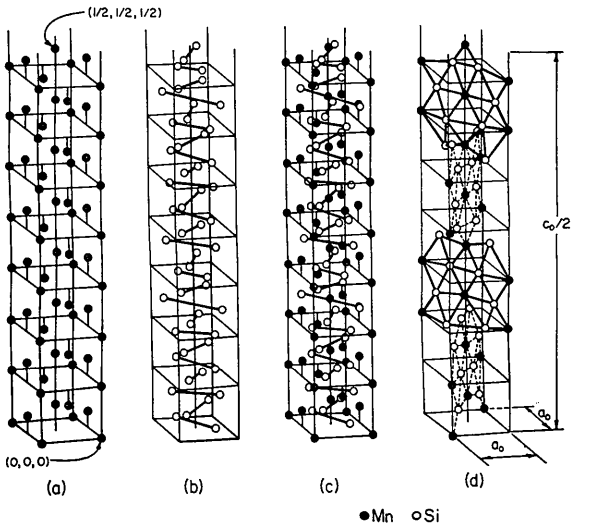


Fig. 1. Sketch of the Mn and Si atoms within one-half a unit cell of $Mn_{15}Si_{26}$ showing stacking of (*a*) Mn subcells, (*b*) Si atom pairs about the central axis, (*c*) Mn and Si atoms, (*d*) pseudo-hexagonal planar array along the (110) and $(1\bar{1}0)$ planes. Solid circles: Mn; open circles: Si.

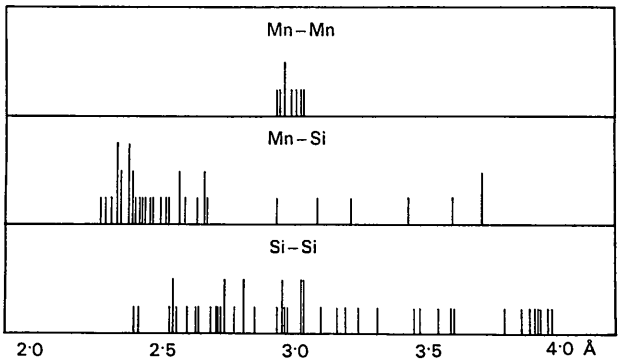


Fig. 2. Histogram showing number and distances of neighbors about the Mn and Si atoms.

Table 3. *Positional and thermal parameters in* $Mn_{15}Si_{26}$*-space group* $I\bar{4}2d$

Standard errors $\times 10^4$ in parentheses.

| | *x* | *y* | *z* | *B* |
|---|---|---|---|---|
| 4 Mn(1) (*a*) | 0 | 0 | 0 | 0·26 |
| 8 Mn(2) (*c*) | 0 | 0 | 0·0653 (4) | 0·18 |
| 8 Mn(3) (*c*) | 0 | 0 | 0·1330 (11) | 0·02 |
| 8 Mn(4) (*c*) | 0 | 0 | 0·1996 (6) | 0·12 |
| 8 Mn(5) (*c*) | 0 | 0 | 0·2669 (8) | 0·21 |
| 8 Mn(6) (*c*) | 0 | 0 | 0·3326 (6) | 0·21 |
| 8 Mn(7) (*c*) | 0 | 0 | 0·4013 (5) | 0·29 |
| 8 Mn(8) (*c*) | 0 | 0 | 0·4644 (3) | 0·09 |
| 16 Si(1) (*e*) | 0·2161 (34) | 0·3445 (42) | 0·0119 (3) | 0·25 |
| 16 Si(2) (*e*) | 0·8515 (49) | 0·1811 (51) | 0·0311 (5) | 0·60 |
| 16 Si(3) (*e*) | 0·3167 (61) | 0·1642 (55) | 0·0480 (4) | 0·32 |
| 16 Si(4) (*e*) | 0·6657 (53) | 0·3434 (53) | 0·0680 (4) | 0·39 |
| 16 Si(5) (*e*) | 0·1591 (50) | 0·3122 (46) | 0·0848 (4) | 0·23 |
| 16 Si(6) (*e*) | 0·7744 (36) | 0·1523 (66) | 0·1063 (2) | 0·46 |
| 8 Si(7) (*d*) | 0·3479 (87) | 0·25 | 0·125 | 0·48 |

Table 4. *Interatomic distances found in* $Mn_{15}Si_{26}$

| Atom 1 | Number of neighbors | Atom 2 | Neighbor distance (Å) |
|---|---|---|---|
| Mn(1) | 4 | Mn | 2·98 |
| Mn(2) | 4 | Mn | 2·93–3·00 |
| Mn(3) | 4 | Mn | 2·96–3·02 |
| Mn(4) | 4 | Mn | 2·93–2·94 |
| Mn(5) | 4 | Mn | 2·98–3·03 |
| Mn(6) | 4 | Mn | 2·96–3·00 |
| Mn(7) | 4 | Mn | 2·96–3·02 |
| Mn(8) | 4 | Mn | 2·94–3·03 |
| Mn(1) | 8 | Si | 2·38–2·42 |
| Mn(2) | 8 | Si | 2·28–2·66 |
| Mn(3) | 8 | Si | 2·30–2·52 |
| Mn(4) | 8 | Si | 2·32–2·63 |
| Mn(5) | 8 | Si | 2·38–2·50 |
| Mn(6) | 8 | Si | 2·32–2·65 |
| Mn(7) | 8 | Si | 2·34–2·51 |
| Mn(8) | 8 | Si | 2·27–2·65 |
| Si(1) | 4 | Mn | 2·37–2·50 |
| Si(2) | 5 | Mn | 2·32–2·65 |
| Si(3) | 5 | Mn | 2·27–2·65 |
| Si(4) | 5 | Mn | 2·32–2·66 |
| Si(5) | 5 | Mn | 2·32–2·63 |
| Si(6) | 4 | Mn | 2·33–2·51 |
| Si(7) | 4 | Mn | 2·37–2·43 |
| Si(1) | 12 | Si | 2·55–3·84 |
| Si(2) | 12 | Si | 2·39–3·91 |
| Si(3) | 12 | Si | 2·39–3·96 |
| Si(4) | 12 | Si | 2·41–3·96 |
| Si(5) | 12 | Si | 2·41–3·92 |
| Si(6) | 12 | Si | 2·63–3·79 |
| Si(7) | 12 | Si | 2·63–3·60 |

Maximum standard errors found ($\times 10^2$) for: Mn–Mn(2); Mn–Si( 4) and Si–Si (5).

### Comparison with other investigations

In order to suggest the best possible structure for this material from our data, a number of comparisons have been made between the three cells; namely $Mn_4Si_7$, $Mn_{11}Si_{19}$ and $Mn_{15}Si_{26}$. The results are summarized in Table 5. The space group for each of these three unit cells is followed by the lattice constants with probable error together with an expression for a fit of the observed and calculated lattice constant data. This fit has been evaluated, as defined by Mueller, Heaton & Miller (1960) by obtaining the difference, $v$, of $\sin^2\theta_{obs}$ and $\sin^2\theta_{calc}$ for each reflection, $i$. Values were then obtained for $\Sigma W_i v_i^2/(n-k-1)\Sigma W_i$, in which $W$ is a weighting term, $n$ is the number of observations and $k$ is the number of variables. Since the smaller the value for this expression the better the agreement, it is apparent that the best lattice constants from both powder and single-crystal data are with the largest cell. Although the probable errors of 0·015 and 0·017 Å on $c$ for this cell are about the same as for the two smaller cells, the apparent error is considerably smaller on a percentage basis of the cell length.

In the next portion of Table 5, the results are given as obtained from a $2\theta$ scan on an X-ray diffractometer of the (00$l$) reciprocal lattice row over the range of 0 to 165° $2\theta$. These observed reflections were indexed based on the three $c$'s obtained from the powder pattern above, and comparisons made of the calculated and observed $d$'s. It can be noted that the average $\Delta d$ is indeed considerably smaller for the largest cell.

The single crystal used on the crystal orienter as described previously was positioned with the $c$ axis nearly coincident with the $\varphi$ axis of the instrument; consequently a change of the $l$ indexing of various reciprocal lattice points as required by each unit cell size had a significant effect upon the $\chi$ angle. This was particularly true since the orientation of the crystal had been established from the least-squares orientation program, B-101, as mentioned previously. In this program the components in the crystal of a unit vector, **A**, which lies along the $\varphi$ axis of the instrument, and the components of a unit vector, **B**, which is perpendicular to **A** and in the $\chi$ plane of the instrument when $\varphi$ is zero are determined from minimized sets of $2\theta$, $\chi$, and $\varphi$ angles from several known $hkl$'s. From these constants the computer generates the instrument angles, $2\theta$, $\chi$, and $\varphi$ for each $hkl$ desired. Hence it was significant to make a comparison of the $\chi_{calc}$ and $\chi_{obs}$ angles. The results obtained from 18 reflections are shown in Table 5.

Comparisons were also made of several film rotation patterns as summarized in Table 5 in order to establish the best repeat distance. These patterns were taken around the $c$ axis and were indexed with the first layer above the zero layer called the 1st, 3rd or 4th layer, respectively, for the three unit cells considered and then observing the deviation from integer values of the remaining layers, either 6 or 7 depending upon the particular film. Indeed the average deviation from a whole number index of $l$ for the three films is least for the largest cell, 0·046, next best for the intermediate cell, 0·280, and poorest for the smallest cell, 0·305. Hence the best indexing for the data is with the largest cell.

Whereas it is true that the differences between the three unit cells are small, each requires a different space group to describe its structure and there are some differences in the atom to atom positions as well as a slight difference in permitted chemical composition for a specific unit cell. For example, if one were to stack 15 of the smallest cells for comparison with a stack of 4 of the largest unit cells each would be the same height involving 60 Mn subcells. Within this framework there would be 210 Si dumbbells (420 Si atoms) within the stacked small cells whereas there would be 208 dumbbells (416 Si atoms) in the stacked large cells, a difference of 4 Si atoms. With the present data it appears impossible to state whether there is indeed only one size of unit cell associated with this approximate Mn–Si composition.

We wish to express our appreciation to Dr J. B. Darby of this Laboratory for suggesting the problem and supplying the samples. We are indebted to Mr J. Gvildys of the Applied Mathematics Division who did the

Table 5. *Some comparisons of data for various sized* Mn–Si *cells*

| Space group | $Mn_4Si_7$ $P\bar{4}c2$ | | | $Mn_{11}Si_{19}$ $P\bar{4}n2$ | | | $Mn_{15}Si_{26}$ $I\bar{4}2d$ | | |
|---|---|---|---|---|---|---|---|---|---|
| | $a$ (Å) | $c$ (Å) | $\frac{\Sigma W_i v_i^2}{(n-k-1)\Sigma W_i}$ | $a$ (Å) | $c$ (Å) | $\frac{\Sigma W_i v_i^2}{(n-k-1)\Sigma W_i}$ | $a$ (Å) | $c$ (Å) | $\frac{\Sigma W_i v_i^2}{(n-k-1)\Sigma W_i}$ |
| Chromium radiation powder pattern – 28 reflections | 5·534 (3) | 17·550 (10) | $3{\cdot}78\times10^{-7}$ | 5·530 (2) | 47·763 (19) | $1{\cdot}94\times10^{-7}$ | 5·531 (1) | 65·311 (15) | $6{\cdot}34\times10^{-8}$ |
| Molybdenum radiation single-crystal – 24 reflections | 5·530 (6) | 17·533 (19) | $5{\cdot}32\times10^{-6}$ | 5·530 (3) | 48·031 (25) | $1{\cdot}27\times10^{-6}$ | 5·530 (2) | 65·562 (17) | $3{\cdot}19\times10^{-7}$ |
| | $\Sigma\lvert d_{obs}-d_{calc}\rvert$ (Å) | Average $\Delta d$ (Å) | | $\Sigma\lvert d_{obs}-d_{calc}\rvert$ (Å) | Average $\Delta d$ (Å) | | $\Sigma\lvert d_{obs}-d_{calc}\rvert$ (Å) | Average $\Delta d$ (Å) | |
| Molybdenum radiation single-crystal (00$l$) scan – 14 reflections | 0·6780 | 0·0484 | | 0·2002 | 0·0143 | | 0·0579 | 0·0041 | |
| | $\Sigma\lvert \chi_{obs}-\chi_{calc}\rvert$ (°) | Average $\Delta\chi$ (°) | | $\Sigma\lvert \chi_{obs}-\chi_{calc}\rvert$ (°) | Average $\Delta\chi$ (°) | | $\Sigma\lvert \chi_{obs}-\chi_{calc}\rvert$ (°) | Average $\Delta\chi$ (°) | |
| Molybdenum radiation single-crystal – 18 reflections | 4·47 | 0·25 | | 1·74 | 0·10 | | 0·58 | 0·03 | |
| | Number of $l$ layers | $\Sigma\lvert\Delta l\rvert$ | Average $\Delta l$ | Number of $l$ layers | $\Sigma\lvert\Delta l\rvert$ | Average $\Delta l$ | Number of $l$ layers | $\Sigma\lvert\Delta l\rvert$ | Average $\Delta l$ |
| Copper radiation single-crystal rotation pattern around $c$ axis | 6 | 1·990 | 0·332 | 6 | 1·846 | 0·308 | 6 | 0·204 | 0·034 |
| | 7 | 1·792 | 0·256 | 7 | 1·357 | 0·194 | 7 | 0·749 | 0·107 |
| | 6 | 1·953 | 0·326 | 6 | 2·026 | 0·338 | 6 | 0·185 | 0·031 |

necessary programming for carrying out this investigation. This work was performed under the auspices of the U.S. Atomic Energy Commission.

### References

ARONSSON, B., LUNDSTRÖM, T. & RUNDQVIST, S. (1965). *Borides, Silicides and Phosphides*, pp. 20, 95, 110. London: Methuen.

BORÉN, B. (1933). *Ark. Kemi Min. Geol.* **11A**, 15.

BUSING, W. R., MARTIN, K. O. & LEVY, H. A. (1962). *A Fortran Crystallographic Least-Squares Program.* Publication ORNL-TM-305, Oak Ridge National Laboratory, Tennessee.

BUSING, W. R., MARTIN, K. O. & LEVY, H. A. (1964). *A Fortran Crystallographic Function and Error Program.* Publication ORNL-TM-306, Oak Ridge National Laboratory, Tennessee.

DARBY, J. B., DOWNEY, J. W. & NORTON, L. J. (1965). *J. Less-Common Metals*, **8**, 15.

FUJINO, Y., SHINODA, D., ASANABE, S. & SASAKI, Y. (1964). *Japanese J. Appl. Phys.* **3**, 431.

*International Tables for X-ray Crystallography* (1962). Vol. III. Birmingham: Kynoch Press.

JEITSCHKO, W. & PARTHÉ, E. (1967). *Acta Cryst.* **22**, 417.

KORSHUNOV, V. A., SIDERENKO, F. A., GEL'D, P. V. & DAVYDOV, K. N. (1961). *Fiz. Metal. Metalloved.* **12**, 277.

MUELLER, M. H., HEATON, L. & MILLER, K. T. (1960). *Acta Cryst.* **13**, 828.

MUELLER, M. H. & KNOTT, H. W. (1965). *Prog. and Abst. Amer. Cryst. Assoc. Meeting*, Gatlinburg, Tennessee: Paper F-2.

SCHWOMMA, O., NOWOTNY, H. & WITTMAN, A. (1963). *Mh. Chem.* **94**, 681.

SCHWOMMA, O., PREISINGER, A., NOWOTNY, H. & WITTMAN, A. (1964). *Mh. Chem.* **95**, 1527.

SLY, W. G. & SHOEMAKER, D. P. (1960). MIFRI: *Two and Three-Dimensional Crystallographic Fourier Summation Program for the IBM-704 Computer*, Department of Chemistry, Massachusetts Institute of Technology, Cambridge, Massachusetts.

VOLLENKLE, A., PREISINGER, A., NOWOTNY, H. & WITTMAN, A. (1967). *Z. Kristallogr.* Accepted for publication.

WITTMAN, A. & NOWOTNY, H. (1965). *J. Less-Common Metals*, **9**, 303.

*Acta Cryst.* (1967). **23**, 555

# A New Method Utilizing a Triangular Grid for the Representation of Preferred Orientation Using Re-Normalized *p* Values Obtained in Inverse Pole Figures

M. J. NASIR AND H. J. BRAY

*Metallurgy Department, John Dalton College of Technology, Manchester, England*

(*Received* 15 *February* 1967 *and in revised form* 20 *March* 1967)

A new method for plotting on one diagram the three inverse pole figures for each of the principal orthogonal sections in a flat rolled, extruded or drawn product has been tested. Such a diagram, designated the *texture triangle*, was found to offer the following advantages: (*a*) A clear idea of the orientation relationship for those planes which give rise to measurable X-ray reflexions can be obtained. (*b*) The change in texture with process variable may be plotted directly on the diagram. (*c*) Texture triangles may be plotted for a series of ideal textures and these may be used for comparative purposes. In this way the texture which is predominant in the specimen may be determined and the severity of the preferred orientation can be calculated in relation to the ideal texture.

## Introduction

Before going into details of the texture triangle an outline of the inverse pole figure method will be given.

In the inverse pole figure technique (Harris, 1952) the diffraction intensities from a preferentially oriented sample are compared with those from a sample having an equal number of grains oriented in all directions. These relative intensities are called *texture coefficients* or *relative pole densities*, $p$, and are expressed mathematically (Morris, 1953; Mueller, 1954) as:

$$p = \frac{I_{hkl}/I^{\circ}_{hkl}}{\frac{1}{n}\sum_{0}^{n} I_{hkl}/I^{\circ}_{hkl}}, \qquad (1)$$

where

$I$ = measured integrated intensity of a given $hkl$ reflexion.

$I^{\circ}$ = calculated intensity for the same $hkl$ reflexion as would be produced by a sample with equal number of grains oriented in all directions.

$n$ = total number of reflexions measured.

$p$ = pole density for a given reflexion.

The quantity $I^{\circ}_{hkl}$ in equation (1) is determined by the equation

$$I^{\circ}_{hkl} = (j)(\mathrm{Lp})(F^2)(e^{-2M}) \qquad (2)$$

where

$j$ = multiplicity factor

Lp = Lorentz–polarization factor